Macromolecules
ARTICLE

Macromolecules **2010**, *43*, 2855–2864 **2855**
DOI: 10.1021/ma100067x

Mechanism of Degradation of Starch, a Highly Branched Polymer, during Extrusion

Wei-Chen Liu,[†] Peter J. Halley,[‡] and Robert G. Gilbert*[,†]

[†]*Centre for Nutrition & Food Sciences, School of Land Crop & Food Sciences, The University of Queensland, Brisbane, Qld 4072, Australia, and* [‡]*Australian Institute for Bioengineering and Nanotechnology, The University of Queensland, Brisbane, Qld 4072, Australia*

Received January 11, 2010; Revised Manuscript Received February 9, 2010

ABSTRACT: An investigation of the mechanisms of degradation of a branched polymer in extrusion was performed using starch as substrate. Starch has the advantage that the distribution of degree of polymerization of individual branches can be readily obtained using a debranching enzyme and also that it does not undergo any reaction except scission during extrusion, thereby aiding mechanistic interpretation. Various starches, containing a range of the highly branched amylopectin component and the much less branched amylose component, were extruded in the presence of water and glycerol as plasticizers with extruder barrel temperatures ranging from 50 °C at the hopper zone through to 140 °C near the die exit. Analysis by size-exclusion chromatography of both whole and debranched samples subject to various levels of extrusion showed that the extrusion degradation process involved preferential cleaving of larger molecules, while causing the size distribution to narrow and converge toward a maximum stable size. This is analogous to a similar effect of shear degradation of droplets in emulsions. It was also found that the susceptibility of polymer molecules to shear degradation is not only dependent on the size of the molecule but also extensively influenced by the branching structure. High branching density and short branch length were associated with higher susceptibility to shear degradation. This is explained by the hypothesis that a short-chain hyperbranched polymer has a relatively inflexible structure, leading to a higher susceptibility to shear scission. The degradation process is not significantly selective toward the length of individual branches when the polymer is in a molten state but it preferentially breaks longer branches when the starch polymer is in a semicrystalline granular form. These inferences are generally applicable and use the additional information from the branch length distribution and absence of side reactions, which is generally not available for synthetic polymers.

Introduction

Thermomechanical processing, such as extrusion, is widely used in polymer processing. Through continuous shearing and heating, it provides means of polymer melting and mixing needed for most plastic shaping applications. High molecular weight polymers (e.g., polypropylene,[1] polystyrene,[2] and starch[3] undergo significant degradation during extrusion. This can change the physical properties of the resulting material, and thus understanding of the shear degradation mechanism during thermomechanical processing is essential for establishing processing−structure−property relationships. This will facilitate the development of functional processing methods that allow the production or recycling of plastics with desirable properties. Although the shear field in an extruder cannot be well characterized, its wide use means that qualitative mechanistic inferences from shear degradation during extrusion will have broad applicability.

This paper explores the degradation mechanism of large highly branched polymers during extrusion, to see if the degradation process has any selectivity toward structural features of the polymer molecule; the properties chosen here are the changes in the distributions of size and of branch length. Starch is constituted entirely of anhydroglucose monomers. All linear chains are linked through α-1,4-glycosidic linkages while branch points are found at α-1,6-glycosidic linkages. Starch comprises polymers of two categories of connectivity: (i) Very high degree of polymerization **amylopectin** ($\sim 10^8$ Da) containing a high density of branches (~5% of glycosidic bonds are α-1,6).[4] The individual branches of amylopectin are normally short with a typical number-average of about 20 to 24 glucose subunits. (ii) Relatively linear **amylose** with approximately 1% branch density and molecular weight ranging from 10^4 to 10^6 Da,[5] with the branches being much longer than in amylopectin. Depending on the plant source, the proportion of amylose and amylopectin can vary. Typically, starch comprises 10−30% amylose and 90−70% amylopectin, but some genetically modified plants can have amylose content up to 85%, while waxy starches are essentially 100% amylopectin.

Starch was chosen as the test subject, because it has a number of significant advantages for the analysis of degradation mechanisms during extrusion, which can shed light on processes in synthetic polymers such as polyethylene and polypropylene. The amylose (long-chain branching) and amylopectin (short-chain branching) components of starch have size and molecular weight distributions which are essentially nonoverlapping, thus enabling the effects of the lengths of branches and overall sizes to be readily distinguished; in polyolefins, there is no significant difference in size distributions of differently branched components. In addition, in the extrusion of polyolefins there is a significant influence of reactions of a variety of unsaturated end-groups (e.g., ref 6), whereas starch comprises largely

*Corresponding author. Telephone: +61 7 3365 409. Fax: +61 7 3365 1188. E-mail: b.gilbert@uq.edu.au.

Published on Web 02/24/2010

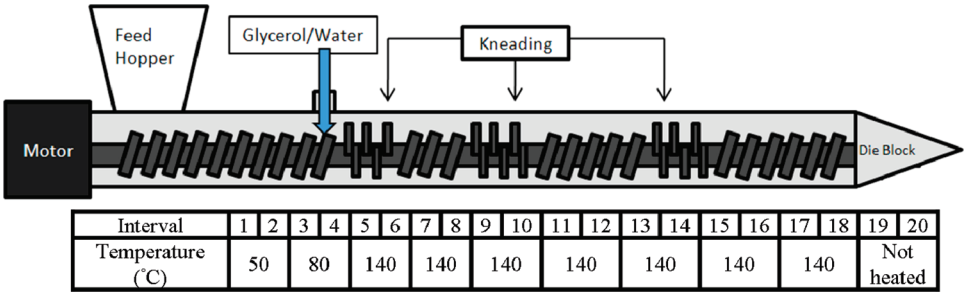

Figure 1. Screw configuration, temperature profile, and interval assignment of the extruder barrel [screw configuration enlarged for clarity; not to scale].

"nonreducing" ends (glucose units with an α-(1,4) linkage to the preceding unit) at the end of each branch and, per whole molecule, a single "reducing" end group (a 6-membered ring with three neighboring −OH groups, which can ring-open to a free aldehyde−keto group); in starch, these end-groups do not undergo reaction in extrusion. Cross-linking,[7−9] side-chain branching and thermo-oxidative reactions[10,11] occur in addition to simple scission in the extrusive degradation of polyolefins, causing an increase in molecular weight and size; the overall size distribution during extrusion is a compound of this increase with the decrease due to simple shear scission. For starch, only simple shear scission (and hence a decrease in molecular weight and size) occurs. Thus, a study of starch enables the mechanisms causing simple shear scission to be studied in isolation. Finally, starch has a particular advantage for the purposes of mechanistic investigation: the molecular weight distribution of individual branches is readily obtained by adding a debranching enzyme, which quantitatively cleaves all branch points.[12] This again provides data which can aid mechanistic interpretation of the degradation process in synthetic polymers, whose branch-length distribution cannot be readily obtained.

Thus, the mechanistic knowledge gained from starch will also be relevant to understanding the shear degradation of synthetic branched polymers.

Starch, besides being the main source of food energy for humans, is also a widely used biodegradable thermoplastic with excellent biodegradability, high availability, a renewable resource, and low cost.[13,14]

The present study uses the changes due to shear degradation of the size distributions of starches of various types. This was implemented by extrusion of starches with different amylose content, collecting samples along the extruder barrel (i.e., with increasing degradation levels), and then characterizing the samples by size exclusion chromatography (SEC, also known as gel permeation chromatography or GPC). This reveals the evolution of the molecular size distribution throughout the course of extrusion. Size distributions have proved useful in providing mechanistic information on branched polymers.[15]

It is important to remember that, with the assumption of universal calibration,[16−19] SEC separates polymers solely by their hydrodynamic volume (V_h), rather than molecular weight. V_h is defined[20] as the volume of a hypothetical sphere that is impenetrable to the surrounding medium displaying in a frictional field the same hydrodynamic behavior as that of the actual polymer. While V_h and molecular weight have a one-to-one relationship for *linear* polymers, this does not hold for complex branched polymers, because different polymers with the same V_h but different branching structures can have different molecular weights. For branched polymers, the results from the SEC are therefore presented in terms of V_h, or equivalently the corresponding hydrodynamic radius R_h, with $V_h = {}^4/_3\pi R_h{}^3$.

In the present study, the results from the size separation were measured by a differential refractive index (DRI) detector to obtain the SEC weight distribution, $w(\log V_h)$. Elution time is converted to hydrodynamic volume using pullulan standards of known Mark−Houwink parameters, as described elsewhere.[21] A problem with this technique is that SEC characterization of amylopectin size distributions cannot avoid some shear scission.[22] While separation by field-flow fractionation (FFF) techniques can reduce scission, as yet there have been no studies of amylopectin with FFF using solvent systems which dissolve all of the starch in a sample (a particular problem with the high-amylose starches which furnish important examples for mechanistic analysis here[23]). For the semiquantitative purposes of the present paper, the presence of shear scission during characterization does not pose any particular difficulty: the semiquantitative interpretation of the resulting (apparent) distributions will be unaffected by this mild scission, because in SEC, large molecules will always elute at shorter elution times, and vice versa.

Experimental Section

Materials. Three varieties of commercially available, genetically modified corn starches (Mazaca, Gelose 50 and Gelose 80) were supplied by Penford Australia Ltd. (Lane Cove, NSW Australia). All starches were chemically unmodified and the amylose contents for these three types of starches were 0%, 55% and 85%, respectively, as measured by Tan et al.[24] using the iodine colorimetric method. Glycerol (99% GC grade), dimethyl sulfoxide (DMSO) (HPLC grade) and lithium bromide (Reagent plus) were from Sigma-Aldrich. Milli-Q water was used in all instances. Two M sodium hydroxide solution (Labscan, Gliwice, Poland), glacial acetic acid (Ajax Finechem, Taren Point, Australia), and isoamylase (Megazyme, Wicklow, Ireland) were used as received.

Sample Preparation. The extrusion processing was performed on a Prism Eurolab 16XL corotating twin−screw extruder (Thermo Electron Corporation, Karlsruhe, Germany) equipped with a 3 mm diameter cylindrical die. The diameter of the barrel bore was 16 mm and the length of the barrel was 640 mm. The screw contains forward conveying elements and kneading elements. The barrel was divided into 20 intervals for sample collection purpose. Intervals 1 to 18 had an equal length of 30 mm per interval while intervals 19 and 20 were the die zones, which had a length slightly shorter than 30 mm. The detailed interval assignment and screw configuration are shown in Figure 1. All starches were fed at a constant rate of 0.312 kg h^{-1} and the screw speed was set at 180 rpm.

The total starch and plasticizer contents were adjusted to 60% starch, 28% glycerol, and 12% water. Plasticizers were introduced to the starch samples in the extruder through an inlet component that was attached to the barrel, as illustrated in Figure 1. The extruder had 10 temperature zones, whose temperatures are also given in Figure 1. Temperature can influence the viscosity of a polymer melt and subsequently change the degradation rate of the polymer during extrusion.[3,25,26] For this reason, the temperature was set at constant 140 °C from intervals 5 to 18 to avoid unwanted effects caused by variation in temperature. The high temperature (140 °C) also facilitated the

gelatinization process of starch, especially high-amylose starches, which in turn enhances the homogeneity of the polymer melt.[27,28]

After approximately 15 min of operation, the torque of the extruder reached a steady state; the extruder was then stopped and starch samples were quickly collected along the barrel. Approximately 200 mg of the samples were collected from intervals 5, 8, 13, 18, and 20.

Debranching of Starch. It is noted that the debranching process is used purely as one of the characterization tools in the analysis of starch samples after extrusion. The samples were enzymatically debranched using isoamylase, an enzyme that exclusively and quantitatively cleaves α-1,6-glycosidic bonds at the branch point. Extruded thermoplastic starch (20 mg) was mixed with 750 μL of water and 50 μL of 2 M sodium hydroxide solution and then completely solubilized in a thermomixer at 95 °C for 30 min. The solution was cooled to room temperature and 32 μL of glacial acetic acid and 100 μL of 1 M sodium acetate solution were added, followed by thorough mixing. Isoamylase (10 μL) and water (1 mL) were subsequently added to the tube and mixed well. The solution was incubated for 24 h in a water bath at 37 °C. After incubation, the mixture was heated to 95 °C for 10 min to denature the enzyme, and then freeze-dried. These conditions lead to the complete debranching of starch.[12,29] As is well-known in the starch community, this leads to a population of two chain lengths after debranching: branches of degree of polymerization 6−100 (typically averaging 20−24) for the short branches comprising the amylopectin fraction, and branches that are more than an order of magnitude longer for the longer branches that comprise the amylose fraction (e.g., refs 29 and 30).

Size Exclusion Chromatography. Size separation was performed on an Agilent 1100 series SEC system (Agilent Technologies, Santa Clara, CA) equipped with a Shimadzu RID-10A differential refractive index detector (Shimadzu Corporation, Kyoto, Japan). The size distributions of fully branched and of debranched starch molecules have quite different ranges of V_h, and thus two column set-ups were used to ensure a clear separation of the molecules. For fully branched starches, the columns used were GRAM 30 and 3000 columns (PSS GmbH, Mainz, Germany) connected in series, which provided separation in the range of 5×10^3 to $\sim 5 \times 10^6$ Da, corresponding to R_h from ~0.5 to ~50 nm. Debranched samples were analyzed by GRAM 30 and 1000 columns connected in series, which had a separation range of 100 to $\sim 10^6$ Da. All columns were maintained at constant 80 °C. As explained elsewhere,[22] there are two potential problems with these SEC data. (a) The fully branched amylopectin will suffer from some shear scission; this will not affect data interpretation in the present case, where the goals are qualitative rather than quantitative. (b) The size scale beyond the calibration range is only semiquantitative, which again does not pose a problem for the present qualitative goals. The range above which calibration and shear scission each become problems is about the same: $R_h > 50$ nm.

The eluent used for SEC characterization comprised 99.5 wt % DMSO and 0.5 wt % LiBr. The ability of this eluent to dissolve starch fully without structural damage has been demonstrated by Dona et al.[31] Schmitz et al. showed that the addition of lithium bromide, which acts as a hydrogen-bond disrupter and prevents retrogradation (crystallization followed by spontaneous precipitation), enhances the solubility of high-amylose starch.[23] The eluent was prepared by dissolving LiBr in DMSO under ultrasonication for 30 min, and then filtered through a 45 μm hydrophilic PTFE membrane under pressure. For each sample, starch extrudate (2 mg) was mixed with 1 mL of the eluent and heated in a thermomixer for approximately 5 h at 80 °C. After the sample was completely dissolved, it was transferred into a SEC vial without filtering, as large amylopectin molecules may be ~1 μm in size, and filtering samples may cause structural damage.

Determination of the Effect of Glycerol on Starch Hydrodynamic Volume. Since starch forms hydrogen bonds with glycerol during extrusion processing, it is possible that after starch is solubilized in DMSO, it could preferentially bind with glycerol rather than DMSO and thus change the V_h of a given starch molecule; this would lead to complications in the qualitative comparison between samples. A test was performed to check whether glycerol affects the V_h of starch. Two samples were made for comparison. The first sample contained 20 mg of Mazaca starch and 13.33 mg of glycerol to make up a mixture that contained 40% glycerol on total weight basis. The second sample contained only 20 mg Mazaca starch. Samples were mixed with 1.5 mL of water and gelatinized in a 100 °C oil bath for 60 min. The gelatinized samples were then dried in an 80 °C oven overnight and characterized by SEC. Results with and without glycerol were compared to see if the presence of glycerol changed the size distribution of starches.

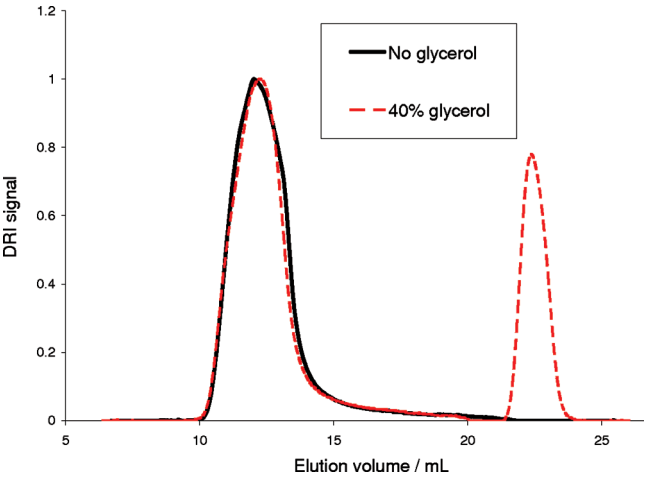

Figure 2. Elution profiles of pure Mazaca starch and Mazaca plasticized with 40% glycerol. The peak at ~22 mL in the glycerol-containing sample is glycerol itself.

Results

Figure 2 shows the SEC elution profile of Mazaca plasticized with 40% glycerol, and the elution profile of Mazaca containing no glycerol. The elution profile of a particular polymer sample is not only dependent on the V_h of the polymer but also dependent on the machine, the column used and which day the experiment is performed. Results expressed in terms of elution time or elution volume are only reproducible if samples are run on the same day with the same SEC machine. Thus, both samples here were run in the same batch. The two elution profiles essentially overlap with each other except for the glycerol peak eluting at ~22.5 mL. This indicates that the protocol used here for starch dissolution will result in all of the glycerol dissociating from starch molecules and thus will give reliable separation in the SEC system. Quantitative comparison can thus be made between pure starch and glycerol-plasticized starch up to a glycerol content of 40%.

Size Distribution of Fully Branched Starch. The normalization of any distribution is arbitrary. All molecular size distributions here are normalized so as to bring out features and to allow qualitative comparison and interpretation. Amylose and amylopectin have slightly different refractive index increments in DMSO/LiBr eluent (the refractive index increments of amylose and high amylopectin rice starch in DMSO/Li at 80 °C are[22] $dn/dc = 0.0689$ and 0.0544 mL g^{-1} respectively at 633 nm). No attempt was made here to take this difference into account, because (1) it makes only a quantitative but not semiquantitative change to the distributions, and (2) for extruded starch, the amylose and amylopectin regions overlap, and thus applying such a correction cannot be implemented. However, because this would make

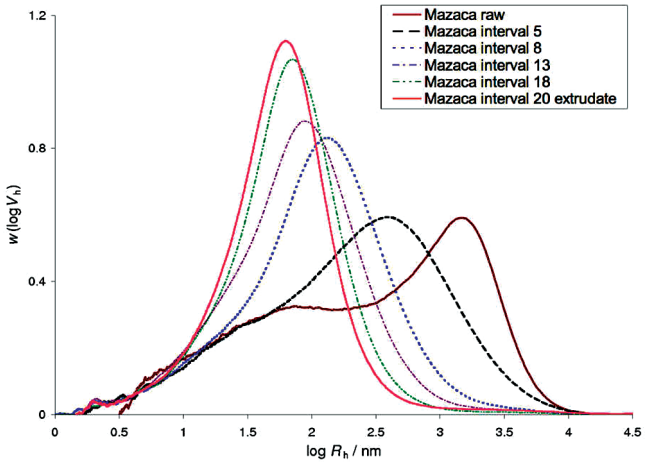

Figure 3. Evolution of the size distribution of fully branched Mazaca starch samples collected along the barrel of the extruder.

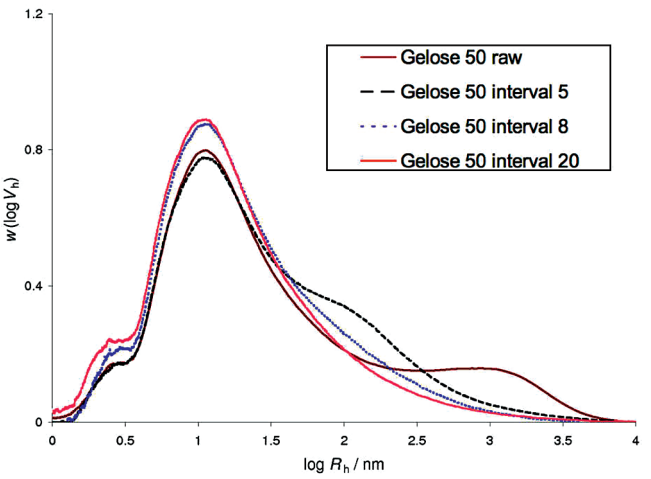

Figure 4. Evolution of size distribution of Gelose 50 starch samples collected along the screw of the extruder.

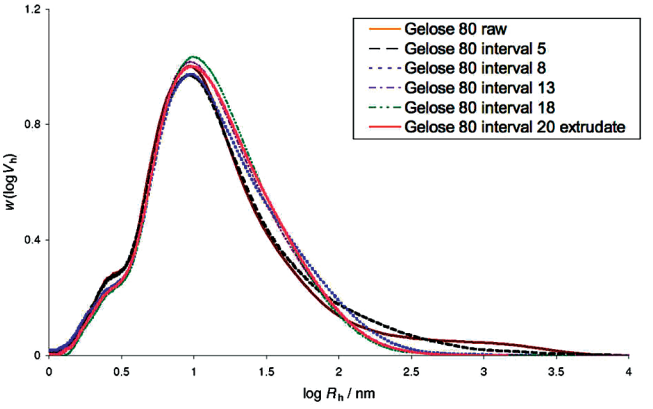

Figure 5. Evolution of size distribution of Gelose 80 samples collected along the screw of the extruder.

only a slight change in the distributions, the relative proportion of amylose and amylopectin is expected to be constant after normalization. Thus, for the fully branched size distributions, normalization was done to make the integral of the curve equal to unity to facilitate identification of any selective degradation process. The amylose and amylopectin fractions were obtained as the areas under the curves as detailed elsewhere.[22]

Figure 3 shows the SEC fully branched size distributions of samples of Mazaca taken progressively along the barrel of the extruder. This figure shows that fully branched Mazaca starch, which contained almost 100% amylopectin, underwent severe degradation during extrusion. Three features can be identified from the evolution profile of Mazaca. First, the size distribution was broad and left-skewed at the start of extrusion and gradually narrowed down as degradation proceeded. Second, the rate of degradation was the highest at the beginning of extrusion and gradually slowed down as the size of the polymer became smaller, implying a size-dependent degradation mechanism. Third, at log (R_h/nm) $\sim$ 1.7, or $R_h \sim 50$ nm, an overlapping region could be identified for the size distributions of Mazaca collected at zone 5, and of raw Mazaca. This overlap shows that molecules below this size did not undergo significant shear degradation during extrusion.

The evolution of Gelose 50 size distribution is presented in Figure 4. The apparent relative proportion of amylopectin is somewhat smaller than 45%, whereas the amylopectin content for this starch has been reported as 45% (see above); this small discrepancy is attributed to amylopectin having a slightly smaller refractive index increment than amylose and also to shear scission of amylopectin during SEC characterization.[22] Similar to the observations for the evolution of size distributions of Mazaca, the amylopectin peak shifted to lower size as extrusion proceeded. An overlap from log (R_h/nm) = 1.7 to 2 ($R_h \sim 50-100$ nm) was found among the unprocessed sample and the sample at zone 20 (extrudate). On the other hand, the unprocessed sample and the sample at zone 5 overlap at the amylose peak maximum region. This indicates that the increase in amylose peak height is due to degraded amylopectin moving under the amylose peak, resulting in a bigger apparent amylose peak, while the amylose peak did not seem to be significantly changed.

The evolution of the size distribution for Gelose 80 is presented in Figure 5. The trend is similar to Gelose 50. The amylopectin peak is smaller than in the Gelose 50 samples, simply because of the lower amylopectin content. The amylose peak, on the other hand, did not seem to vary significantly throughout the extrusion process.

Size Distributions of Debranched Starch. Debranched starches are completely linear glucan chains, and therefore their distributions can be presented in the form of molecular weight distributions; this is easier to comprehend than the alternative of presenting data for a linear polymer in terms of R_h. It should also be noted that SEC data suffer from some degree of band broadening. This effect may change the details of the resulting molecular weight distribution and mask important features. A deconvolution technique developed by Castro et al.[32] was adopted in present study to convert the SEC data in terms of elution volume and pullulan standards to convert from size to actual molecular weight distributions of linear glucans with some correction for band-broadening (deconvolution). In this method, a "standard" is used comprising a sample of debranched starch whose true (number) molecular weight distribution has been accurately measured using fluorophore-assisted capillary electrophoresis (FACE).[33,34] FACE can resolve individual oligomers with baseline separation up to degrees of polymerization (DP) $X \sim 80$. The SEC distribution of this same sample is then used to find the band-broadening function, typically an exponentially modified Gaussian,[35] applicable to that particular data set. The parameters so obtained can then used to deconvolute other samples over the same range of DP. This procedure also yields the Mark−Houwink parameters in the eluent employed.

Figure 6 shows the FACE data for a sample of debranched regular maize starch (Penford Australia Ltd.), and Figure 7 shows the measured SEC distribution for the same sample. FACE directly gives the (debranched) number distribution $N_{de}(X)$, the number of (debranched) chains of DP X (trivially related to molecular weight M by multiplying by 162, the molecular weight of anhydroglucose monomer, plus the molecular weight of a water molecule). The number distribution is related to the corresponding SEC weight distribution $w_{de}(\log X)$ by:[36,37]

$$w_{de}(\log X) = X^2 N_{de}(X) \quad \text{(only valid for linear polymers)} \tag{1}$$

For a linear (unbranched) molecule such as debranched starch (but not for branched ones such as whole starch), size (as V_h) and molecular weight are related through the Mark−Houwink equation:

$$V_h = \frac{2KM^{1+\alpha}}{5 \quad N_A} \tag{2}$$

where N_A is Avogadro's constant. Determination of the Mark−Houwink parameters K and α will be discussed below. Figure 7 also shows the calculated broadened SEC distribution calculated using the true number distribution of Figure 6, convoluted with a band-broadening function whose parameters were least-squares fitted to give the best match between this calculated distribution and that obtained from SEC (the latter of course being subject to band-broadening).

This fit yields not only the particular broadening parameters applicable to the particular SEC setup, but also the Mark−Houwink parameters for linear starch in the eluent (DMSO/0.5% LiBr at 80 °C): $K = 0.0150$ mL g^{-1} and $\alpha = 0.743$. The band broadening parameters and Mark−Houwink parameters obtained can then be used to deconvolute samples run in the same SEC experiment. However, the data used here go to much higher molecular weights than the range covered by the debranched "standard". For this reason, the Mark−Houwink parameters were used to convert size to molecular weight without correcting for band-broadening.

Figures 8 and 9 show the debranched molecular weight distribution (MWD) of Mazaca samples presented both as the SEC weight distribution $w_{de}(\log X)$ and the number distribution, as $\ln N_{de}(X)$. There are mechanistic reasons for presenting debranched data in this logarithmic form for native starch,[30] which may or may not be useful for the present case of processed and degraded starch: although the SEC and number distributions contain the same information, certain features may be more apparent when the data are presented in one form or the other. The number distribution was calculated from the SEC weight distribution

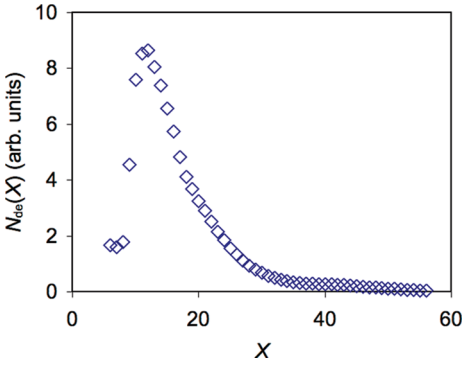

Figure 6. FACE data for a sample of debranched regular maize starch. FACE gives the (debranched) number distribution $N_{de}(X)$.

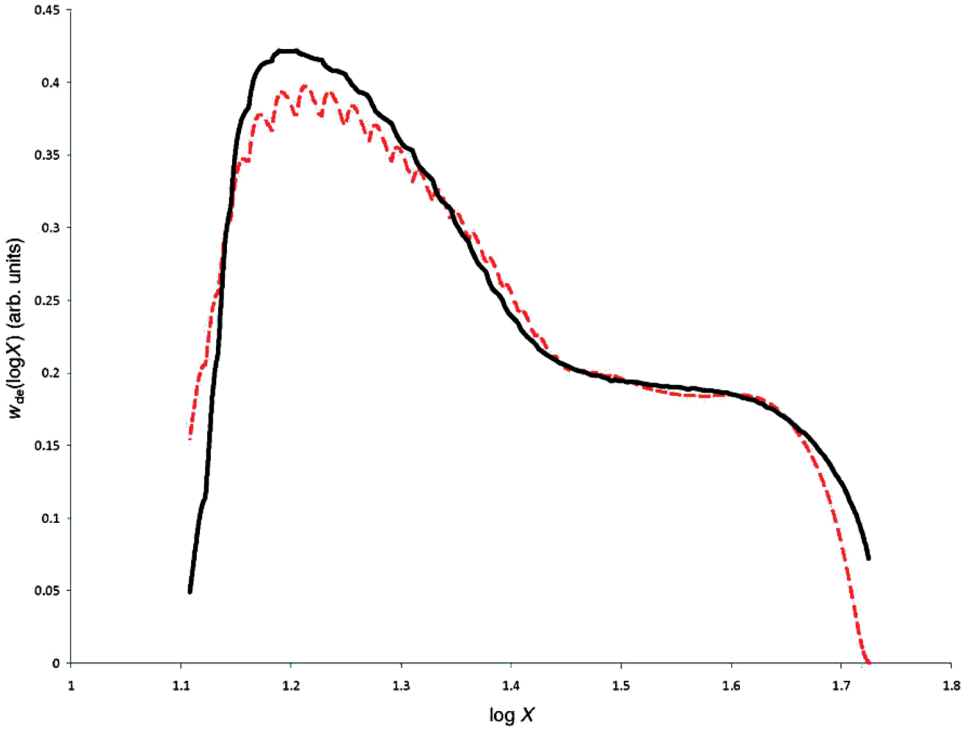

Figure 7. Full line: experimental SEC distribution for the same sample as Figure 6. Broken line: number distribution of Figure 6 converted to the corresponding SEC distribution using eq 1 and convoluted with a band-broadening function whose parameters were least-squares adjusted to give the best match between the two distributions. The convolution integral to take account of broadening converts discrete peaks from individual DPs in the FACE data to small local maxima.

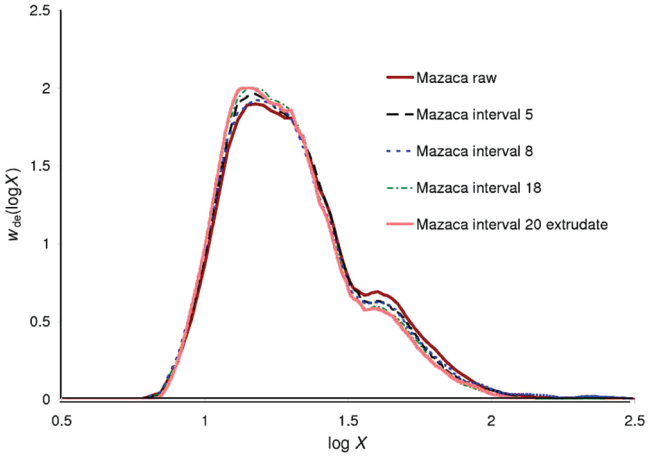

Figure 8. Debranched MWD of Mazaca along the barrel of the extruder, as the SEC weight distribution, $w_{de}(\log X)$.

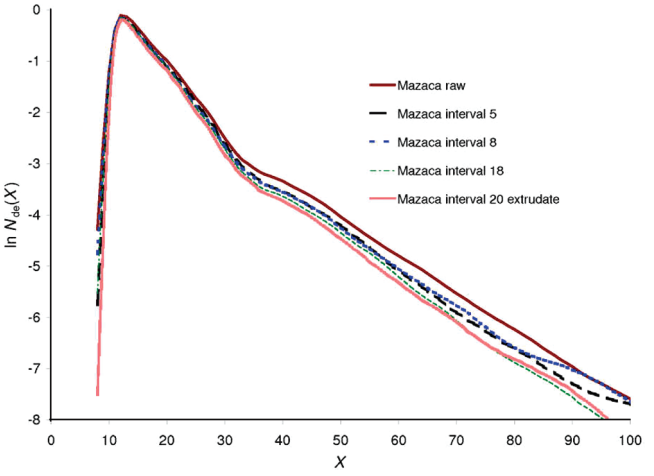

Figure 9. Data of Figure 8, presented as ln $N_{de}(X)$.

through eq 1. All debranched distributions show a bimodal distribution in the amylopectin region (smaller chains), with the smaller and larger components coming from chains that are confined to a single lamella and those that traverse more than one lamella, as is well-known for starch (e.g., ref 30). The amylose component has several maxima, again as seen in the literature.[29]

While significant degradation was observed for whole-molecule Mazaca samples, the debranched molecular weight distributions of Mazaca throughout the course of extrusion show very little difference over the relevant range of log X: from 0.5 to 2.5. The entire distribution moved gradually to lower M during the course of extrusion, but the shape of the distribution remained the same. The same observation was seen in the number distribution. As the two methods of presenting the data show similar trends, only the SEC w_{de}-(log X) will be used hereafter.

The debranched MWDs for Gelose 80 are given in Figure 10. Similar to Mazaca, there is no significant change in the MWD from zone 5 to zone 20, except for a slight reduction in the molecular weight throughout the entire distribution. However, for samples collected at zone 5, a reduction in peak intensity was observed in the highest molecular weight region (log X from 2.8 to 4) accompanied by an increase in peak intensity in the medium molecular weight region (log X from 1.8 to 2.8). This suggests that shear causes selective scission of longer branches.

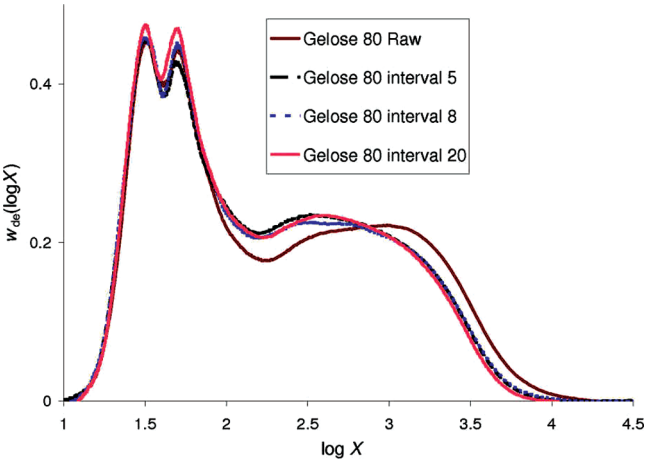

Figure 10. Debranched MWD of Gelose 80 along the barrel of the extruder presented as the SEC weight distribution, $w_{de}(\log X)$.

Interpretation. From Figure 3, it is apparent that amylopectin undergoes significant degradation throughout the course of extrusion. If random whole-molecule scission were to occur in this process, one would expect the entire molecular size distribution to shift to a lower size, accompanied by broadening of the width of the distribution. However, in the present study, the degradation *narrowed* the size distribution. This suggests that the degradation mechanism is not random but instead has some selectivity toward structural features of the polymer, which will now be discussed.

The susceptibility of a polymer chain to shear degradation is strongly influenced by its molecular size. As shown in Figure 3, the size distribution of raw Mazaca starch was left-skewed (more large molecules), but as extrusion proceeded, the distribution gradually became more symmetrical. This shows that over the same intervals (same shear history, residence time, and temperature), larger molecules have a higher probability of being sheared, which then results in more medium-size and small molecules. Thus, the distribution becomes less skewed as degradation proceeds. Moreover, it is clear that the changes in size distribution become much less significant after interval 13, which indicates a fast decline in degradation rate with respect to the decrease in molecular size. The observations are in accordance with the idea that the degradation process is selective toward size and preferentially operates on large molecules. Similar results have been reported in the literature.[3,38,39] However, since the viscosity of the polymer melt reduces as the average size of the polymer decreases, the reduction in viscosity may also contribute to the lowering of the overall degradation rate. As a result, the decrease in degradation rate is probably a combined effect of reduction in melt viscosity and the reduction of sizes of individual molecules, the former also deriving from the latter (e.g., a feedback loop or self-dampening mechanism)

Maximum Stable Size and Size Distribution of Fragments. Since the degradation process preferentially operates on large polymers, leaving small polymer chains relatively intact, it leads to a narrowing of the size distribution, as presented in Figure 3. Because the degradation rate decreases as the size of polymer decreases, eventually the polymer chains would be sheared down to a maximum stable size. This is similar to the concept of droplet breakup under shear in an emulsion system[40−42] and in SEC-induced shear scission of highly branched polymers.[22] That is, for a given shear environment or extrusion condition, no shear degradation can take place for polymer chains smaller than this

maximum stable size, and one would expect the size distribution to narrow and converge toward the maximum stable size as degradation proceeds further. The reason for the existence of a maximum stable size for shear scission of branched polymers in extrusion is presumably the same as that for shear degradation of branched polymer solutions in SEC.[22] As noted by Cave et al.,[22] shear scission of droplets is opposed by the viscosity of the liquid in the discrete phase and by interfacial tension. With a highly branched polymer in an extruder, the equivalent of viscosity within a droplet is the resistance of the interconnected branches to energy dissipation with an external force. The equivalent to interfacial tension is the thermodynamic tendency of the chain to retain its approximately spherical equilibrium conformation against an external force.

This concept of maximum stable size is an approximation, and in actuality one would expect a relatively narrow distribution around an average maximum stable size, rather than a perfectly monodisperse size distribution.

Supporting this concept, it is seen that the size distributions of raw Mazaca and Mazaca collected at interval 5 overlapped below $\log(R_h/\text{nm}) \sim 1.7$, as shown in Figure 3. This overlapping region indicates no shear degradation had occurred below this R_h over the intervals 1 to 5. Thus, $R_h \sim 10^{1.7} \sim 50$ nm can be taken as the maximum stable size for the extrusion conditions in this study. The size distribution of the final extrudate also has its peak close to $R_h \sim 50$ nm, which supports the maximum stable size hypothesis.

It is also seen that the maximum stable size is slightly different for different starches (Figures 3 and 4). The maximum stable size is expected to be different for samples with different amylose content, for the following reason. Increasing amylose content increases the viscosity of the polymer melt and hence increases the maximum shear stress. This will consequently lead to a smaller maximum stable size. Consistent with this, the 100% amylopectin Mazaca starch has a maximum stable size around $\log(R_h/\text{nm}) \sim 1.7$ and the high-amylose Gelose 50 starch has its maximum stable size somewhat below this value.

It is of interest to determine whether the shear degradation during extrusion preferentially cuts the polymers at the outer chains or close to the center of the chain. The differences in location of the scission in the overall molecule can lead to very different property changes of the resulting materials. If the outer chains were cleaved from the parent chain, the fragments would be expected to be orders of magnitude smaller than the original polymer (provided the individual branch length is short, which is indeed the case for amylopectin) and the resulting molecular size distribution would have a bimodal distribution, consisting of one peak of parent chains and another peak of the sheared fragments with much smaller size. On the other hand, if the bond breakage were close to the center of the chain, the fragments would be of intermediate size, comparable to the original polymer chain, and the resulting size distribution would shift to lower size but would not exhibit an additional peak. This is sketched in Figure 11.

From Figure 3, it is seen that the evolution of size distribution for Mazaca is not bimodal. Furthermore, the overlap between size distributions of the unprocessed sample and the sample at interval 5 below $\log(R_h/\text{nm}) = 1.7$ ($R_h \sim 50$ nm) also shows that no significant amount of small fragments was produced during extrusion. Therefore, the shear degradation process in extrusion is most likely to fragment the polymer close to the center, which results in fragments of intermediate size. This is reasonable, as the shear stress on a small portion of a large molecule will be much less than on two moieties of similar size, an effect which has previously been pointed out for linear polymer chains.[43]

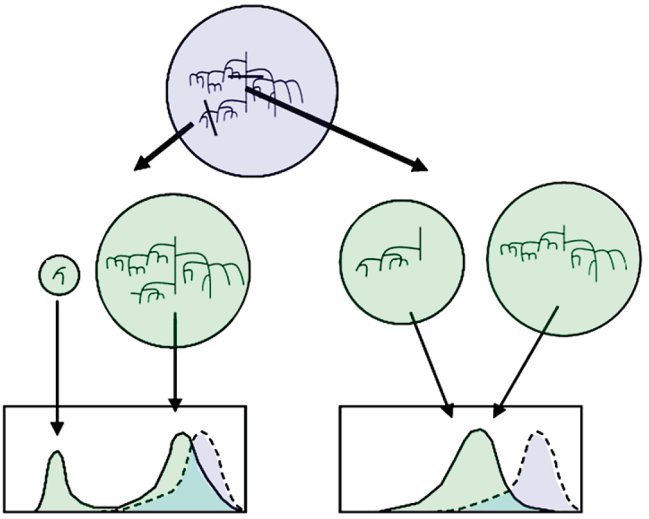

Figure 11. Different bond breaking positions during the extrusion of intact starch molecules lead to different size distributions. If bond rupture occurred at the outer part of the molecule, the original distribution (dotted line) would be sheared to two separated peaks (solid line) consisting of the parent chains and the fragments; if bond rupture were close to the center of the molecule, the bimodal distribution would not be seen.

Branching Structure and Selective Scission. It has been suggested in the literature that amylopectin is more susceptible to shear degradation than amylose.[3,44,45] Under the extrusion conditions adopted in present study, we found that the size distribution of amylopectin undergoes severe changes while the size distribution of amylose does not seem to vary notably. The results are consistent with the literature, and also with the "maximum stable size" mechanism established for shear scission of droplets. However, whether the susceptibility of amylopectin to scission is solely due to its large size or due to both its size and branching structure has not been fully addressed. The evolution of Gelose 50 size distribution in the present study provides some useful insights to this question. In Figure 4, the amylopectin component was shear-degraded and gradually moved to lower size regions as extrusion progressed, similar to the results in Figure 3. Eventually, the amylopectin chains were fragmented to a size comparable to amylose, and merged into the amylose peak, resulting in an increase in the relative proportion of the apparent amylose component. Although the degraded amylopectin and amylose can no longer be distinguished beyond this point, two implications are found from this evolution of size distribution.

First, the size distribution of original Gelose 50 overlaps with the sample collected at interval 5 at the amylose peak region ($\log(R_h/\text{nm})$ from 0.6 to 1.4, $R_h \sim 4-25$ nm). This indicates that, under the same extrusion conditions and over the same intervals, amylose is not significantly degraded, while amylopectin starts to undergo fast degradation. In Figure 5 it is seen that the evolution of the size distribution for the sample with the highest amylose content, Gelose 80, does not show significant changes throughout the extrusion process, which supports the hypothesis that amylose does not undergo significant degradation during extrusion.

Second, the size distribution of unextruded Gelose 50 also overlaps with that of the final extrudate in the medium to high R_h amylose region from $\log(R_h/\text{nm}) = 1.7$ to 2 ($R_h \sim 50-100$ nm). This indicates that there was no amylopectin in this region.

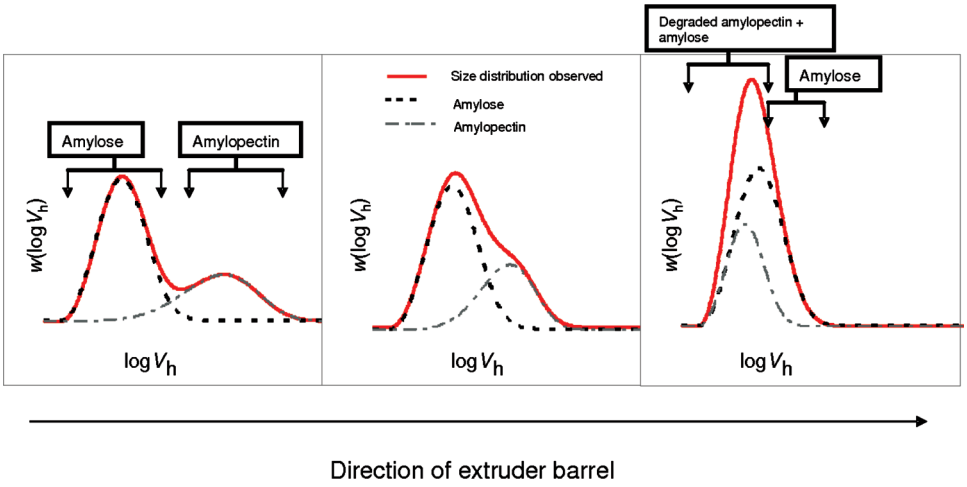

Figure 12. Sketch of the evolution of the amylose and amylopectin components and the superposition of the two components throughout the course of extrusion.

As sketched in Figure 12, the observation suggests that as extrusion proceeds, amylopectin molecules are continuously degraded, and at the end of extrusion processing, the fragments are a size comparable to amylose molecules. Thus, the peak representing amylopectin completely passed through the high R_h amylose region and we see the trace of the original size distribution in the high amylose region from $\log(R_h/\text{nm}) = 1.7$ to 2 before and after extrusion. This implies that, for the same size, amylose is still more stable than amylopectin under a given shear environment.

This effect is most likely due to the differences in branching structure of the two starch components. Amylopectin comprises a large number of relatively short branches connected together to form a hyperbranched structure; when one part of the molecule is subjected to a shear force, the relatively low flexibility of a short branch means that the shear force cannot be easily spread throughout the entire molecule. On the other hand, sparsely branched amylose comprises a small number of long branches, and these long branches can withstand a higher extent of deformation without translating the shear force to the entire molecule. As a result, because of the hyperbranched connectivity of amylopectin, it is relatively inflexible under shear compared to amylose, which leads to higher susceptibility to shear degradation.

The shear degradation process in extrusion is consequently not only selective toward size but also selective toward the branching structure of molecules. The results from this study provide the first evidence to show that higher branching density is also associated with the high susceptibility of amylopectin to shear degradation.

Some work has been conducted on degradation of polyethylene and polypropylene during extrusion where scission of long chain branches in polyethylene[46] and chain scission of polypropylene[10] has been reported, but as stated in these papers more detailed knowledge of macromolecular branching structure and degradation chemistry needs to be understood in explaining the degradation processes. The present study provides useful insight into these processes.

Debranched Molecular Weight Distribution and Shear Degradation Mechanism. The evolution of the debranched distribution (the branch or chain-length distribution) provides information about the changes of individual branches during extrusion. This gives indications to whether the rupture of the glycosidic bond preferentially takes place at branches with certain lengths, or alternatively if it is independent of branch length.

Figures 8 and 9 show that the debranched Mazaca distributions are very similar to each other throughout the course of extrusion. While the entire distribution shifted slightly toward the low molecular weight region as extrusion proceeded, there is no significant change in the shape of the distribution, nor is there any selective reduction in proportion of chains with certain lengths. The results suggest that the actual breaking of glycosidic bonds within the chain is not a selective process. That is, glycosidic bonds in long branches have the same probability of being broken as short branches under extrusion. However, since the debranched molecular weight distributions are very similar to each other, there is a possibility that the shear degradation of starch during extrusion preferentially cleaves off branch points (e.g., shear degradation is essentially an incomplete debranching process). In this case, the distribution of individual branch lengths would remain the same. Nevertheless, only a small number of bond cleavages would be needed to create a drastic reduction in the R_h of a highly branched molecule. Given that amylopectin is highly branched and that individual branches have relatively low degree of polymerization, a small number of bond breakages of individual branches would not significantly change the debranched molecular distribution, while selectively breaking only the branch points (α-1,6-linkages) would not change the debranched structure at all.

The SEC weight distributions of debranched Gelose 80 from interval 5 to interval 20, as shown in Figure 10, show similar trends to Mazaca. However, there is a notable reduction in the proportion of highest molecular weight chains (log X from 2.8 to 4) accompanied by an increase in the weight proportion of medium molecular weight chains (log X from 1.8 to 2.8) between raw Gelose 80 and Gelose 80 collected at zone 5. One possible explanation for this feature could be that, as plasticizers were introduced from zone 3 onward, the starch before zone 3 would not have been gelatinized, i.e. would retain some of the semicrystalline structure in the native starch. This observation suggests that ungelatinized and gelatinized starches have different degradation mechanisms under shear.

The question arises as to whether amylose could undergo shear scission purely because its branches are long, as distinct from being a much smaller molecule than amylopectin (which as explained is susceptible to shear scission because it is so large and relatively inflexible, being comprised only of short highly connected branches). However, the branches in

amylose, although long (say, DP ~ 500), are much shorter than those in synthetic polymers which susceptible to shear scission.[46] Thus, the individual branches of amylose will not be strongly prone to shear scission, although as noted above there can be some preferential scission of longer chains. This hypothesis is supported by the observation that the amylose component does not show significant shear degradation.

Conclusions

The evolutions of molecular size distribution for both fully branched and debranched maize starches have been studied throughout the course of extrusion to understand the degradation mechanism of branched polymers during thermomechanical processing, and to identify any degradation processes that are selective toward structural features of the polymer. The results show significant shear degradation of the amylopectin component, and the changes in size distribution suggests the degradation mechanism preferentially operates on large molecules. However, it is not just the large size which causes susceptibility to shear scission. Amylopectin is not only larger than amylose, but also it has much shorter branches; the hyperbranched connectivity of amylopectin gives it a relatively inflexible structure, reducing the maximum deformation it can withstand without breaking. It was also found that the concept of maximum stable size, similar to droplet breakup in an emulsion system, is applicable here: below the maximum stable size, little shear degradation occurs for given extrusion conditions. The observation that the size distribution of amylopectin molecules narrowed and converged toward this maximum stable size as extrusion proceeded is due to both selective scission and the maximum stable size concept.

The mechanism for scission of the polymer chains is believed to preferentially take place close to the center of the molecule, as suggested in the literature for other polymer systems.[43] This is inferred from the absence of a bimodal distribution after extrusion. Furthermore, from the evolution of debranched molecular weight distributions, the degradation was found not to be selective toward individual branch lengths for gelatinized starch during extrusion.

For starch, (1) one can directly obtain the distribution of branch lengths, which is not possible for most synthetic branched polymers, (2) starch contains two components with very different branching structures (amylose and amylopectin), and (3) the degradation of starch during extrusion involves only simple shear scission, without the additional complications of cross-linking, branching and end-group reactions which occur in addition to shear scission in polyolefin extrusion. These points enable the present study to furnish new mechanistic information germane to the shear degradation of synthetic branched polymers. In addition, since the lengths of branches have an effect on the digestibility of starch in food (e.g., the amount of "resistant starch"[47−49]), the fact that it is amylopectin, not amylose, which suffers the most shear degradation and that this is because of branching structure as well as size also has nutritional relevance in starch processing.

Future work will focus on examining the effects of screw configuration and specific mechanical energy (SME) on degradation to better understand the effects of processing on extrusion degradation.

Acknowledgment. R.G.G. gratefully acknowledges the financial support of a Discovery Grant from the Australian Research Council (DP0985694). We greatly appreciate the expertise of Dr. Richard Cave for the SEC measurements.

References and Notes

(1) Ying, Q. C.; Yong, Z.; Yong, L. *Makromol. Chem.—Macromol. Chem. Phys.* **1991**, *192*, 1041–1058.
(2) Arisawa, K.; Porter, R. S. *J. Appl. Polym. Sci.* **1970**, *14*, 879–896.
(3) Davidson, V. J.; Paton, D.; Diosady, L. L.; Larocque, G. *J. Food Sci.* **1984**, *49*, 453–458.
(4) Buleon, A.; Colonna, P.; Planchot, V.; Ball, S. *Int. J. Biol. Macromol.* **1998**, *23*, 85–112.
(5) Hizukuri, S.; Takagi, T. *Carbohydr. Res.* **1984**, *134*, 1–10.
(6) Pinheiro, L. A.; Chinelatto, M. A.; Canevarolo, S. V. *Polym. Degrad. Stab.* **2004**, *86*, 445–453.
(7) Caceres, C. A.; Canevarolo, S. V. *Polim.—Cien. Tecnol.* **2009**, *19*, 79–84.
(8) Kealy, T. *J. Appl. Polym. Sci.* **2009**, *112*, 639–648.
(9) Scaffaro, R.; La Mantia, F. P.; Botta, L.; Morreale, M.; Dintcheva, N. T.; Mariani, P. *Polym. Eng. Sci.* **2009**, *49*, 1316–1325.
(10) Hinsken, H.; Moss, S.; Pauqueta, J.-R.; Zweifel, H. *Polym. Degrad. Stab.* **1991**, *34*, 279–292.
(11) Pock, E.; Kiss, C.; Janecska, A.; Epacher, E.; Pukanszky, B. *Polym. Degrad. Stab.* **2004**, *85*, 1015–1021.
(12) Bertolini, A. C. *Starches: characterization, properties, and applications*; Bertolini, A. C., Ed.; CRC Press: Boca Raton, FL, 2010.
(13) Gross, R. A.; Kalra, B. *Science* **2002**, *297*, 803–807.
(14) Avella, M.; De Vlieger, J. J.; Errico, M. E.; Fischer, S.; Vacca, P.; Volpe, M. G. *Food Chem.* **2005**, *93*, 467–474.
(15) Hernández, J. M.; Gaborieau, M.; Castignolles, P.; Gidley, M. J.; Myers, A. M.; Gilbert, R. G. *Biomacromolecules* **2008**, *9*, 954–965.
(16) Grubisic, Z.; Rempp, P.; Benoit, H. *J. Polym. Sci., Polym. Lett. Ed.* **1967**, *5*, 753–759.
(17) Grubisic, Z.; Rempp, P.; Benoit, H. *J. Polym. Sci., Part B: Polym. Phys.* **1996**, *34*, 1707–1714.
(18) Hamielec, A. E.; Ouano, A. C. *J. Liquid Chromatogr.* **1978**, *1*, 111–120.
(19) Kuge, T.; Kobayashi, K.; Tanahashi, H.; Igushi, T.; Kitamura, S. *Agric. Biol. Chem.* **1984**, *78*, 2375–2376.
(20) Jones, R. G.; Kahovec, J.; Stepto, R.; Wilks, E. S.; Hess, M.; Kitayama, T.; Metanomski, W. V. *Compendium of Polymer Terminology and Nomenclature. IUPAC Recommendations 2008*; Jones, R. G., Kahovec, J., Stepto, R., Wilks, E. S., Hess, M., Kitayama, T., Metanomski, W. V., Ed.; Royal Society of Chemistry: Cambridge, U.K., 2009.
(21) Gray-Weale, A.; Cave, R. A.; G.Gilbert, R. *Biomacromolecules* **2009**, *10*, 2708–2713.
(22) Cave, R. A.; Seabrook, S. A.; Gidley, M. J.; Gilbert, R. G. *Biomacromolecules* **2009**, *10*, 2245–2253.
(23) Schmitz, S.; Dona, A. C.; Castignolles, P.; Gilbert, R. G.; Gaborieau, M. *Macromol. Biosci.* **2009**, *9*, 506–514.
(24) Tan, I.; Torley, P. J.; Halley, P. J. *Carbohydr. Polym.* **2008**, *72*, 272–286.
(25) Guha, M.; Ali, S. Z.; Bhattacharya, S. *J. Food Eng.* **1997**, *32*, 251–267.
(26) Diosady, L. L.; Paton, D.; Rosen, N.; Rubin, L. J.; Athanassoulias, C. *J. Food Sci.* **1985**, *50*, 1697–1699.
(27) Liu, H. S.; Yu, L.; Xie, F. W.; Chen, L. *Carbohydr. Polym.* **2006**, *65*, 357–363.
(28) Liu, H. S.; Yu, L.; Simon, G.; Zhang, X. Q.; Dean, K.; Chen, L. *Carbohydr. Res.* **2009**, *344*, 350–354.
(29) Ward, R. M.; Gao, Q.; de Bruyn, H.; Gilbert, R. G.; Fitzgerald, M. A. *Biomacromolecules* **2006**, *7*, 866–876.
(30) Castro, J. V.; Dumas, C.; Chiou, H.; Fitzgerald, M. A.; Gilbert, R. G. *Biomacromolecules* **2005**, *6*, 2248–2259.
(31) Dona, A.; Yuen, C.-W. W.; Peate, J.; Gilbert, R. G.; Castignolles, P.; Gaborieau, M. *Carbohydr. Res.* **2007**, *342*, 2604–2610.
(32) Castro, J. V.; Ward, R. M.; Gilbert, R. G.; Fitzgerald, M. A. *Biomacromolecules* **2005**, *6*, 2260–2270.
(33) Morell, M. K.; Samuel, M. S.; O'Shea, M. G. *Electrophoresis* **1998**, *19*, 2603–2611.
(34) O'Shea, M. G.; Samuel, M. S.; Konik, C. M.; Morell, M. K. *Carbohydr. Res.* **1998**, *307*, 1–12.
(35) Baumgarten, J. L.; Busnel, J. P.; Meira, G. R. *J. Liquid Chromatogr. Relat. Technol.* **2002**, *25*, 1967–2001.
(36) Shortt, D. W. *J. Liquid Chromatogr.* **1993**, *16*, 3371–3391.
(37) Clay, P. A.; Gilbert, R. G. *Macromolecules* **1995**, *28*, 552–569.
(38) Baud, B.; Colonna, P.; Della Valle, G.; Roger, P. In *Starch—Advances in Structure and Function*; Barsby, T. L., Donald, A. M., Frazier, P. J., Eds.; Royal Society of Chemistry: Cambridge, U.K., 2001; pp 40−44.
(39) Cai, W.; Diosady, L. L.; Rubin, L. J. *J. Food Eng.* **1995**, *26*, 289–300.
(40) Arai, K.; Konno, M.; Matunaga, Y.; Saito, S. *J. Chem. Eng. Jpn.* **1977**, *10*, 325–330.

(41) Janssen, J. M. H.; Meijer, H. E. H. *J. Rheol.* **1993**, *37*, 597–608.
(42) Cristini, V.; Guido, S.; Alfani, A.; Blawzdziewicz, J.; Loewenberg, M. *J. Rheol.* **2003**, *47*, 1283–1298.
(43) Basedow, A. M.; Ebert, K. H. *Adv. Polym. Sci.* **1977**, *22*, 83–148.
(44) DellaValle, G.; Colonna, P.; Patria, A.; Vergnes, B. *J. Rheol.* **1996**, *40*, 347–362.
(45) van den Einde, R. M.; van der Goot, A. J.; Boom, R. M. *J. Food Sci.* **2003**, *68*, 2396–2404.
(46) Ono, K.; Yamaguchi, M. *J. App. Polymer Sci.* **2009**, *113*, 1462–1470.
(47) Berry, C. S. *J. Cereal Sci.* **1986**, *4*, 301–314.
(48) Sievert, D.; Pomeranz, Y. *Cereal Chem.* **1989**, *66*, 342–347.
(49) Gidley, M. J.; Cooke, D.; Darke, A. H.; Hoffmann, R. A.; Russell, A. L.; Greenwell, P. *Carbohydr. Polym.* **1995**, *28*, 23–31.